DOI: 10.18721/JCSTCS.13302
УДК 004.946

A FAST ALGORITHM FOR VISUAL MODELING OF RICE LEAF CELLS

W. Yi, Y. Zhao

Jiangxi Agricultural University,
Nanchang, China

In order to rapidly construct a visual model of rice leaf cells, the authors employed modeling tools of computer aided geometric design (CAGD): curve and surface. Rice mesophyll cells are an object of the study. In virtue of the Bernstein basis function properties and convex combination optimization, this work reconstructs the computation graph of the de Casteljau algorithm to model rice leaf cells, and C++ programming language and OpenGL rendering library are used to establish the visual model of cells. The theoretical results indicate that the control variables of curve and surface shape can be increased by revising affine combination coefficient through the polynomial space of the Bernstein basis function expansion. In addition, the results suggest that the convex combination optimization approach reduces the calculated time complexity of cytoskeleton interpolation points from O(n2) to O(n). The experimental results show that the convex combination algorithm has a significant advantage in terms of computation speed over the de Casteljau algorithm for each 200 interpolation points of the cytoskeleton. In view of the characteristics of close arrangement, regular shape, and large quantity of plant cells, the method proposed in this study has the ability to provide a feasible technical route and a rapid expression for visual modeling of plant cells.

Keywords: rice leaf cells, fast algorithm, visualization, CAGD, parameter curve.

Citation: Yi W., Zhao Y. A fast algorithm for visual modeling of rice leaf cells. Computing, Telecommunications and Control, 2020, Vol. 13, No. 3, Pp. 17–30. DOI: 10.18721/JCSTCS.13302

БЫСТРЫЙ АЛГОРИТМ ВИЗУАЛЬНОГО МОДЕЛИРОВАНИЯ КЛЕТОК РИСОВЫХ ЛИСТЬЕВ

В. И, И. Чжао

Jiangxi Agricultural University,
Nanchang, China

Для быстрого построения визуальной модели клеток рисового листа используются инструменты компьютерного геометрического проектирования (Computer Aided Geometric Design, CAGD) – «кривые» и «поверхности». В качестве объекта исследования взяты клетки мезофилла риса. На основании свойств базисной функции Бернштейна и оптимизации выпуклых комбинаций создаётся вычислительный граф алгоритма де Кастельжо для моделирования клеток рисового листа, а для построения визуальной модели клеток используется язык программирования C++ с библиотекой рендеринга OpenGL. Теоретические результаты показывают, что управляющие переменные кривой и формы поверхности могут быть увеличены путем пересмотра коэффициента аффинной комбинации через полиномиальное пространство разложения базисной функции Бернштейна. Кроме того, полученные результаты свидетельствуют о том, что подход оптимизации выпуклой комбинации позволяет уменьшить время сложного расчета точек

интерполяции цитоскелета с O(n2) до O(n). Экспериментальные результаты демонстрируют, что алгоритм выпуклой комбинации имеет значительное преимущество с точки зрения скорости вычислений по сравнению с алгоритмом де Кастельжо для каждых 200 точек интерполяции цитоскелета. Учитывая особенности близкого расположения, правильной формы и большого количества растительных клеток, предложенный в данном исследовании метод способен обеспечить технологическую схему и быстрое выражение для визуального моделирования растительных клеток.

Ключевые слова: клетки рисовых листьев, быстрый алгоритм, визуализация, CAGD, кривая параметров.

Ссылка при цитировании: И В., Чжао И. Быстрый алгоритм визуального моделирования клеток рисовых листьев // Computing, Telecommunications and Control. 2020. Vol. 13. No. 3. Pp. 17–30. DOI: 10.18721/JCSTCS.13302

Introduction

The leaves are the main vegetative organs that perform crucial functions, such as photosynthesis and water transpiration, etc. Therefore, exploring the leaf morphology not only provides scientific guidance for improving the leaf's external morphology and increasing the internal functioning efficiency, but also has important research significance for improving the rice yield and quality. The research community has studied the rice leaf morphology by using genetic breeding technique, and discovered the gene that affects the leaf width, angle of inclination, and degree of curling. However, these studies mainly focus on a single gene regulation. Currently, it is still unclear whether all the genes affecting the whole rice leaf morphology formation are discovered and if there are any interactions between gene regulation networks [1]. This forms the basis of obstacles in leaf morphology modeling based on the gene regulation network.

In addition, few studies show that the cell morphology and quantity are the major factors that influence the formation of plant leaves, and the effect of mechanical force on cells is the main cause of the morphology formation [2–6]. On the basis of this theory, in this paper, we attempt to take the cell as the smallest research unit and use visualization technology to perform computer modeling for leaf local cells. This is done to provide computer aided design (CAD) support for rice leaf 3D morphology formation research.

Relevant works

The CAD technology can simulate a biological test which is either expensive or not easy to realize on computer platforms. It is an effective quantitative biological research method [7–12]. The interior of a rice leaf is observed using an optical microscope. It has plenty of cells: epidermis, mesophyll and vascular. The epidermis cells are closely arranged in a long geometrical shape. A mesophyll cell is a regular polygon with a thin wall and large intercell spaces. The vascular cells are in a slender geometrical shape [13]. It is known that the geometrical shapes of plant leaf cells are simple, and rapidly reconstructing the visual model is the research key of the CAD technology.

In computer aided geometric design (CAGD), the main research focus is to use the curve parameter equation to describe the object's skeleton morphological information [14–16], which has two aspects. One is using simple and low-order curve to approximate smooth and graceful curve according to the object's geometrical characteristics. The other is using numerical calculations and algorithm optimization to improve the rendering speed of the geometric model. The relevant studies in the first aspect are as follows. Some researchers adopted the Möbius transform to construct a quartic rational parabolic Pythagorean-Hodograph (PH) curve to satisfy C^2 continuous CAD design [17, 18]. In an attempt to satisfy a flexible design of curve inflection points, Lu et al. proposed indirect PH method to guarantee G^1 continuous Hermite interpolation according to the geometrical characteristics of Bessel control polygon [19]. Khan et al. used

the convergent Lupaş Bernstein operators proved by Korovkin theorem to control the free deformation of the curve and the surfaces [20]. Kirmani et al. searched for the parameters that satisfy spline 3rd-order polynomial on the basis of Caputo fractional derivative factors, and thus fits the object's geometrical shape [21]. Asghar and Mustafa proposed a general formula for tensor product surfaces subdivision of one and two variables in order to reconstruct high order continuity and realistic vision of the object's geometrical model [22].

In recent years, the advancement in the applications of visualization technology imposes higher requirements for the calculation efficiency of geometric modeling. For example, Nuntawisuttiwong and Dejdumrong reduced the interpolation computing time by transforming Newton-Lagrange polynomials calculation into a linear algorithm [23]. Beccari and Casciola solved the curve that satisfied C^1 continuity by using the integral recursion method. This algorithm is beneficial for improving the storage efficiency of the vector diagram [24]. As the robustness of the integral recursion method is not clear, in order to break through the calculation dependence, Toshiiwal et al. constructed a space curve crossing the entirety of multiple order splines. This method realizes multiple order basis function splines by using the existing B spline [25]. As for subdivision algorithm, Hussain et al. generated a 5 points approximate subdivision mode through variable parameters, and introduced a shape parameter to construct different geometric graphs [26]. In addition, few scholars executed a binary subdivision algorithm after estimating the depth of curve and surface using a data algorithm. The research presented by Shahzad et al. shows that this method provides a significant improvement [27]. Besides, some studies inherited the advantages of endpoints and convex combination of the Bernstein basis function. Woźny and Chudy presented a recursive algorithm to reduce the time complexity of curve solution to linearity [28]. In this work, the second aspect is regarded as foundation, and geometric modeling of rice mesophyll cells as an example. The authors studied rapid solution algorithm of cell's geometric skeleton to improve the visual expression speed of leaf cells.

Materials and methods

The authors selected hybrid rice seed "Gangyou 6366". First, the seed is soaked in water for 10 min. Secondly, 100 plump seeds are selected and placed evenly on the double absorbent paper in a sprouting box, and water is added until the absorbent paper is fully saturated. Finally, the sprouting box is placed in a manual climatic box (MGC-250Hp, Shanghai Yiheng) to accelerate germination. The environmental parameters are: 25 °C temperature, 50 % humidity, 16 hours of light per day. After five days of the experiment, a rice leaf is randomly selected to be transacted at the middle segment. Since leaf epidermis and mesophyll cells are thin and allow the transmission of light, the contours of cells are not clear. Hence, the leaf segment to be observed is placed into absolute ethyl alcohol and heated to 70 °C for 1 hour. Then, Motic BA210 Digital Microscope (100x objective lens, 3-million-pixel charge coupled device (CCD)) is used to shoot the mesophyll cells of this leaf material. Three mesophyll cells are taken as visual modeling objects, with the shapes as shown in Fig. 1. Each closed full line frame is a mesophyll cytoskeleton, and dotted points are prepared curve control points.

The morphological structural changes are difficult to observe to the naked eye from microcosmic perspective, therefore computer simulation technology is used to express cell evolution and group competition [29]. Rational Bézier curve and surface geometric modeling technology is widely applied in CAGD [30]. However, as compared to rigid body objects, the plant leaf cells are large in quantity. Moreover, the cells are deformed due to biophysical mechanical effects. The rapid reconstruction and correct expression of a geometric shape model for a plant cell are the key points of visual simulation. On this basis, three research steps are presented in this work. As shown in Fig. 2, first, rational Bézier geometric modeling computation graph and designing algorithms of de Casteljau recursion and convex combination optimization are proposed, respectively. Secondly, both classes are compared on the basis of computational efficiency, and the faster algorithm is selected to establish a shape mesh model of a rice mesophyll cell. Finally, C++ and OpenGL graphics rendering library are adopted to establish a cell's

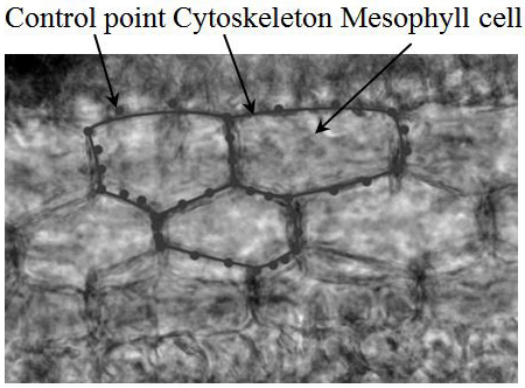

Fig. 1. Geometry of the discolored mesophyll cells

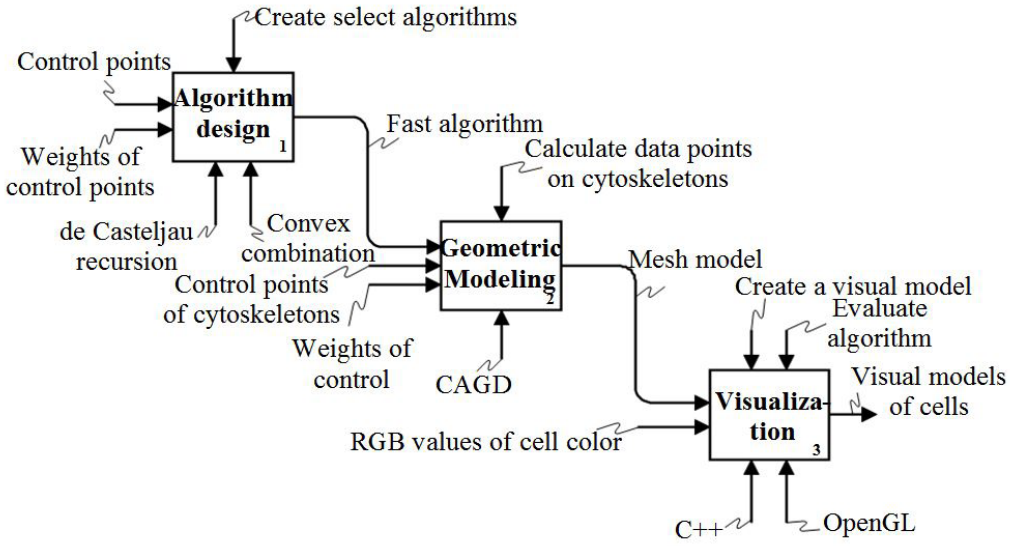

Fig. 2. Main methods and technical roadmap

visual model to estimate the algorithm time complexity. In the aforementioned steps, the rapid geometric modeling algorithm of cells is the main issue to be studied.

The CAGD object modeling is transformed to the evaluation of object geometric data points for control points set $\{ p_i \in \mathbb{R}^3 | \, i = 0, 1, .., n\}$ and the corresponding weights set $\{\omega_i \in \mathbb{R}^+ | \, i = 0, 1, ..., n\}$. The rational Bézier curve calculation is presented in (1) and (2):

$$r^n(t) = \sum_{i=0}^{n} p_i \beta_i^n(t) \tag{1}$$

$$\beta_i^n(t) = \frac{\omega_i^n B_i^n(t)}{\sum_{i=0}^{n} \omega_i^n B_i^n(t)}. \tag{2}$$

Where (2) extends to the n^{th} order rational function space $\beta^n = \text{span}\{\beta_i^n(t) \mid i = 0, 1, .., i\}$, and $\beta_i^n(t)$ satisfies the following properties:

(i) Non-negativity: for arbitrary $\omega_i > 0$ and $t \in [0, 1]$, it has: $\beta_i^n(t) \geq 0$;

(ii) Unit decomposability: $\sum_{i=0}^{n} \beta_i^n(t) = 1$; and

(iii) Endpoint property: $\beta_i^n(0) = \delta_{i0}$, $\beta_i^n(1) = \delta_{in}$, in which δ is Kronecker symbol.

Proof: As this space is based on classic Bernstein basis function $\beta_i^n(t)$, according to the non-negativity of Bernstein basis function, when curve control vertex weight $\omega_i > 0$, it is evident that $\beta_i^n(t) \geq 0$.

As the denominator i in (2) is irrelevant to the numerator, when the numerator adds the same sum operation, the cancellation of numerator with denominator is 1.

According to endpoint properties of $\beta_i^n(t)$, it can test that when $t = 0$ and $i = 0$, $\delta_{i0} = 1$; and when $t = 1$ and $i = n$, $\delta_{in} = 1$, respectively.

To sum up, the rational basis function $\beta_i^n(t)$ satisfies the properties (i)-(iii).

Assuming that quartic rational Bézier curve's control vertex and weights set $\{ p_i ; \omega_i \mid i = 0, 1, 2, 3\}$ denote the local geometric information of the cytoskeleton, we obtain the curve's polynomial according to (1)-(2):

$$r^3(t) = p_0\beta_0^3 + p_1\beta_1^3 + p_2\beta_2^3 + p_3\beta_3^3 = \frac{(1-t)^3\omega_0}{\omega} p_0 + \frac{3t(1-t)^2\omega_1}{\omega} p_1 + \\ + \frac{3t^2(1-t)\omega_2}{\omega} p_2 + \frac{t^3\omega_3}{\omega} p_3, \tag{3}$$

where $\omega = (1-t)^3\omega_0 + 3t(1-t)^2\omega_1 + 3t^2(1-t)\omega_2 + t^3\omega_3$.

Assuming $\lambda_0 = \frac{(1-t)^3\omega_0}{\omega}$, $\lambda_1 = \frac{3t(1-t)^2\omega_1}{\omega}$, $\lambda_2 = \frac{3t^2(1-t)\omega_2}{\omega}$, and $\lambda_3 = \frac{t^3\omega_3}{\omega}$.

The above polynomial coefficient $\lambda_0 + \lambda_1 + \lambda_2 + \lambda_3 = 1$. The aforementioned relation shows that when the given fixed point $t \in (0, 1)$, the data point $r^3(t)$ on the quartic rational Bézier curve is obtained by the affine combination of control points set $\{ p_i \}$. λ is the combination coefficient, and the data point is inside the polygon enclosed by the control points set. When $t = 0$ or 1, β_i^3 satisfies the endpoint property $r^3(0) = p_0$, and $r^3(1) = p_3$.

According to (3), denominator ω expression uses the function of affine combination $L(t) = a^n(1 - t) + b^n t$, that is, $\omega = l_1(t)\ l_2(t) ...\ l_n(t)$, in which a^n and b^n represent the adjacent combinations' coefficients λ_i^n and λ_{i+1}^n, respectively. The aforementioned process can be expressed as the following computation graph, as shown in Fig. 3.

The computation graph displays the data point calculation process of the rational Bézier curve based on de Casteljau recursive algorithm. In a similar way, (3) is generalized to the n^{th} order rational Bézie curve for solution. The recursive calculation is shown below:

$$r_i^k = \begin{cases} r_i^0 = p_i\ ,\ \lambda_i^0 = \omega_i \\ \dfrac{\lambda_i^k(1-t)}{\lambda_i^k(1-t) + \lambda_{i+1}^k t} r_i^{k-1} + \dfrac{\lambda_{i+1}^k t}{\lambda_i^k(1-t) + \lambda_{i+1}^k t} r_{i+1}^{k-1}, \end{cases} \tag{4}$$

where $k = 1, 2, ..., n$; $i = 0, 1, ..., n–k$. The recursive process of the cytoskeleton data point algorithm is presented in Listing 1.

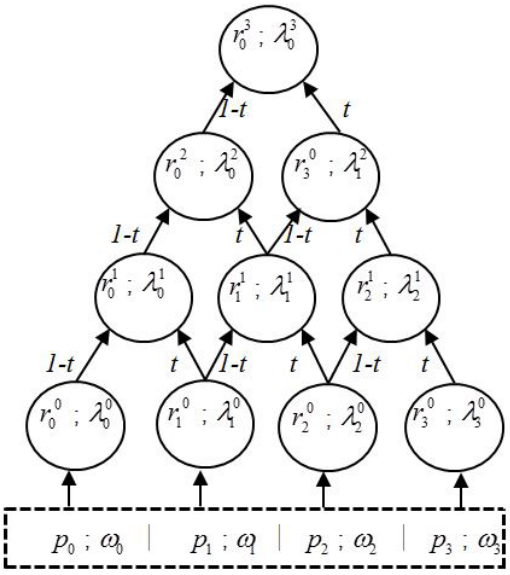

Fig. 3. Computation graph of rational curve modeling based on de Casteljau recursive algorithm

Input: int n, **float** t, **vector < Point3 >** p, **vector < float >** ω;
Output: vector < Point3 > *cytoskeleton*;

1. **Initialize:** $i = 1$, $j \leftarrow 0$, $r = p$, $\lambda = \omega$;
2. **While** i **less than or equal to** n
3. **While** j **less than or equal to** $n-i$
4. $u \leftarrow (1-t) * \lambda_j$;
5. $v \leftarrow t * \lambda_{j+1}$;
6. $\lambda_j \leftarrow u+v$;
7. $u \leftarrow u / \lambda_j$;
8. $v \leftarrow 1-u$;
10. $r_j \leftarrow u * r_j + v * r_{j+1}$;
11. *cytoskeleton=push_back*(r_j);
12. $j \leftarrow j+1$;
13. $i \leftarrow i+1$;

Listing 1. Calculate points of cytoskeleton based on de Casteljau recursive algorithm (Algorithm 1)

According to curve control vertex convex combinations of curves and surfaces, the research idea is rewritten [28]. The de Casteljau recursive computation graph of cytoskeleton evaluation can be rewritten as the optimized convex combination form as shown in Fig. 4.

Thus, the local geometric shape of cytoskeleton can be rewritten as another form s^k, which satisfies the recursive convex combination of (5):

$$s^k = \begin{cases} s^0 = p_0, \ d^0 = 1 \\ \left(1-d^k\right) s^{k-1} + d^k p_k \end{cases}, \tag{5}$$

where $k \in [0, 1, ..., n]$, $d^k = \dfrac{\lambda^k d^{k-1} t(n-k+1)}{\lambda^{k-1} k(1-t) + \lambda^k d^{k-1} t(n-k+1)}$.

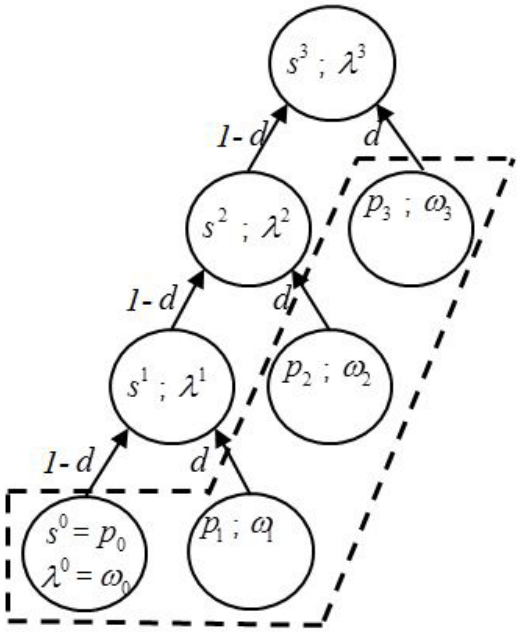

Fig. 4. Computation graph of rational curve modeling based on convex combination optimization

Proof: According to (1), the k-order rational basis function expression can be obtained as follows:

$$d^k = \sum_{i=0}^{k} p_i \frac{\lambda^i B^i(t)}{\sum_{i=0}^{k} \lambda^i B^i(t)}. \tag{6}$$

When $k = 0$, $d^k = 1$.

When $k > 0$, (6) can be written as

$$\sum_{i=0}^{k} p_i \frac{\lambda^i B^i(t)}{\sum_{i=0}^{k} \lambda^i B^i(t)} = \sum_{j=0}^{k-1} p_j \frac{\lambda^j B^j(t)}{\sum_{j=0}^{k} \lambda^j B^j(t)} + p_k \frac{\lambda^k B^k(t)}{\sum_{j=0}^{k} \lambda^j B^j(t)}. \tag{7}$$

According to (1), (2), and basis function property (ii), (7) is substituted into the control vertex and summation formula to obtain: $S^k = S^{k-1}(1-d^k) + p^k d^k$.

$n = k$ and $n = k-1$ are substituted into (2), respectively. (8) and (9) are obtained as

$$d^k(t) = \frac{\lambda^k B^k(t)}{\sum_{k=0}^{k} \lambda^k B^k(t)} = \frac{\lambda^k B^k(t)}{\sum_{k=0}^{k-1} \lambda^{k-1} B^{k-1}(t) + \lambda^k B^k} \tag{8}$$

$$d^{k-1}(t)=\frac{\lambda^{k-1}B^{k-1}(t)}{\sum_{k=0}^{k-1}\lambda^{k-1}B^{k-1}(t)}. \tag{9}$$

(9) is substituted into (8), and (10) is obtained as

$$d_k=\frac{\lambda_k d_{k-1}B_k(t)}{\lambda_{k-1}B_{k-1}(t)+\lambda_k d_{k-1}B_k(t)}. \tag{10}$$

When $0 < k \le n$, Bernstein basis function is used to expand (10), and we get

$$d^k=\frac{\lambda^k d^{k-1}t(n-k+1)}{\lambda^{k-1}k(1-t)+\lambda^k d^{k-1}t(n-k+1)}. \tag{11}$$

Thus, (5) is proved.

The convex combination algorithm of cytoskeleton data point evaluation is expressed as presented in Listing 2.

Input: int n, **float** n, **vector < Point3 >** p, **vector < float >** ω ;
Output : vector < Point3 > *cytoskeleton*;

1. **Initialize**: $d \leftarrow 1.0$, $m \leftarrow 1.0-t$, $s \leftarrow p_0$, $\lambda \leftarrow \omega$, *cytoskeleton* = *push_back*(s), k=1;
2. **While** k **less than or equal to** n
3. $d \leftarrow \lambda_k * d * t * (n-k+1)$;
4. $d \leftarrow d / (\lambda_{k-1} * k * m + d)$;
5. $s \leftarrow (1-d) * s_{k-1} + d * p_k$;
6. **If** k **equal to** $n-1$
7.
8. *cytoskeleton* = *push_back*(s);
   $k \leftarrow k+1$;

Listing 2. Calculate points of cytoskeleton based on convex combination optimization (Algorithm 2)

Experimental results

In this work, the configuration parameters of computer hardware include Intel(R) Core(TM)i5-8400 CPU @2.80GHz 2.80GHz, 8G memory, 64-bit Windows 10 Pro, and Intel(R)UHD Graphics 630 NVIDIA GeForce GTX 1050 GPU. The authors used C++ programming design language and OpenGL 2.2 graphics rendering library. The geometric modeling involves processes of CPU and GPU calculations. In view of CPU operations, firstly C++ is adopted to realize the geometric shape mesh point evaluation of Algorithm 1 and Algorithm 2. Then, these values are successively bound to Vertex Buffer Object (VBO), Element Buffer Object (EBO), and Vertex Array Object (VAO), and then imported to the OpenGL graphics rendering library for GPU operations. Finally, after the processing of vertex and fragment shaders, a visual model is displayed

on the computer screen. In order to verify the modeling efficiency of Algorithm 1 and Algorithm 2 in CAGD, we perform modeling experiments on the curve and the surface in terms of the two algorithms. As presented in Table 1 and Table 2, the position vector of curve control vertices and the position matrix of surface control vertices are provided.

Table 1

Control points of curve modeling, cm

p_0	p_1	p_2	p_3
[0.0, 3.0, 0.0]	[2.0, 7.0, 0.0]	[4.0, 7.0, 0.0]	[6.0, 3.0, 0.0]

Table 2

Control vertices of surface modeling, cm

p_{ij}	0	1	2	3
0	[0.0, 0.0, 2.0]	[0.0, 1.0, 2.0]	[0.0, 2.0, 2.0]	[0.0, 3.0, 2.0]
1	[2.0, 0.0, 0.0]	[2.0, 1.0, 0.0]	[2.0, 2.0, 0.0]	[2.0, 3.0, 0.0]
2	[4.0, 0.0, 0.0]	[4.0, 1.0, 0.0]	[4.0, 2.0, 0.0]	[4.0, 3.0, 0.0]
3	[6.0, 0.0, 2.0]	[6.0, 1.0, 2.0]	[6.0, 2.0, 2.0]	[6.0, 3.0, 2.0]

Without loss of generality, the value of interpolation points t is 40, and $\omega_i = 1$. The geometric shape visual results of Algorithm 1 and Algorithm 2 are shown in Fig. 5. The control polygon of Algorithm 2 is obtained by the convex combination of Algorithm 1. The curves and surface shapes of the desired values are similar. However, the geometric curvature obtained by Algorithm 2 is larger than the geometric shape of Algorithm 1.

The theoretical time complexities of two aforementioned algorithms are $O(n^2)$ and $O(n)$. As the number of interpolation points in geometric modeling tasks is small, the calculation of the modeling results is completed within 1 ms. In order to further test the calculation efficiencies of two algorithms in rice leaf cells modeling, the three adjacent mesophyll cells marked in Fig. 1 are selected in this study. For each cell,

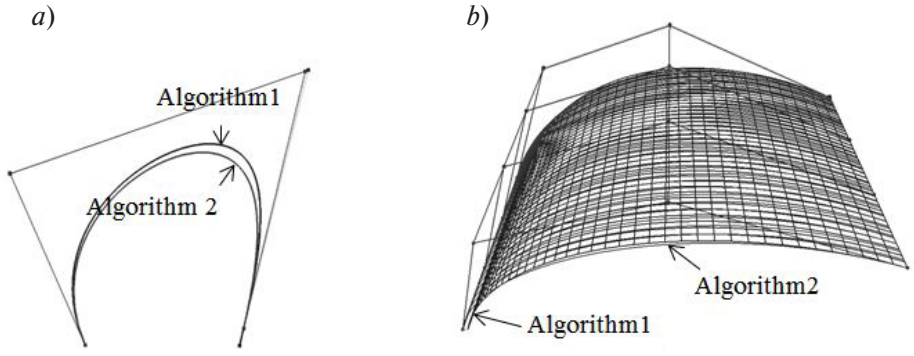

Fig. 5. Geometric modeling of the two algorithms: *a* – curves; *b* – surface

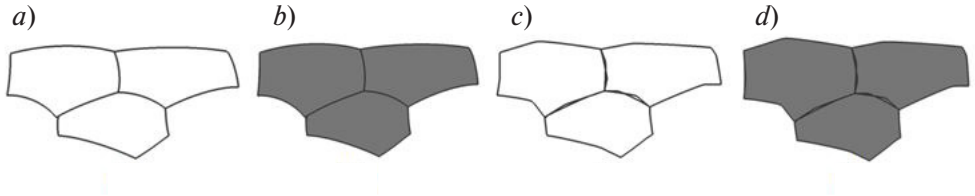

Fig. 6. Simulated results of cells: *a* – cytoskeleton; *b* – Filled color cells; *c* – cells deformation on weight changes; *d* – Filled color of cells deformation

we adopt C^0 continuous curve combination. In the process of this experiment, it sets 48,000 rendering points of cell contour. The achieved results are presented in Fig. 6.

Fig. 6 *a*, *b* presents visual images of three cells when all the given control vertexes' weights $\omega_i = 1$. When the control vertexes adjacent to cells are assigned with different weights, the cells deform. The corresponding results are shown in Fig. 6 *c*, *d*. The computational time comparison of two algorithms on the geometric modeling of three adjacent rice mesophyll cells indicates that Algorithm 2 is 8 ms faster than Algorithm 1.

Discussions

The study on cell morphology by quantitative method needs to be supported by high-precision and high-tech devices. The development and application of biological microscopy enable the researchers to collect the geometric information of the microscale objects. A cell is the smallest living system with relatively "short" growth cycle. Traditional biological tests often use biochemistry and genetic methods to study some profiles of the cell living system to obtain the relevant information of cell growth. However, we are challenged with a comprehensive information integration problem, which is to study the operation of cell systems through the integration of multiple systems' profile knowledge. The virtualization and visualization technologies aim at establishing algorithms and models on computer platform to simulate and observe the real-world objects as well as to predict the evolution. In addition, it also helps researchers to build up the cell growth information models at the biochemical, physical and presentation layers. Moreover, it effectively integrates each layer's cell growth information [2, 4].

CAGD usually uses polynomial to approximate the curve and the surface. The space formed by these polynomials is obtained by the affine combination l_n of the Bernstein basis function, i.e., $l_n = a_n(1 - t) + b_n t$. Therefore, in view of Bézier type curve and surface, the improved algorithms are classified into two types. The first type introduces new combination coefficient variables to increase the degree of shape control freedom. For example, the combination coefficient (a_n, b_n) is replaced with $(\lambda_n a_n, \lambda_n b_n)$. The other type uses convex combination properties to change the combination ways of polynomials, thus reducing the computations [28]. The plant cell walls make the cells with the same type connect closely [31]. In this work, the rice mesophyll cells are taken as example, and the studies of two aspects are integrated. In addition, this work also discusses the visualization technology of plant call at presentation layer. Moreover, it studies a set of rapid expression methods in view of plant cell visual modeling. This method designs the affine combination algorithm of rational shape control factor λ, and emphatically analyses the time complexities of these two algorithms. The modeling calculation time of cell parameter curve and surface is shown in Fig. 7.

In the process of cell visualization based on curve modeling, as shown in Fig. 7 a, for every 200 interpolation points, the execution time of Algorithm 1 and that of Algorithm 2 are 6.551724 millisecond and 2.711598746 millisecond, respectively. The execution speed of Algorithm 2 is more significant in terms of statistics than that of Algorithm 1. In addition, the *p*-value of the *t*-test result of the two groups of data is 2.5117e-06 (significantly smaller than 0.01). However, in the process of surface modeling, as shown in Fig. 7 b, for the same interpolation points, the execution speed of Algorithm 2 is faster than that of Al-

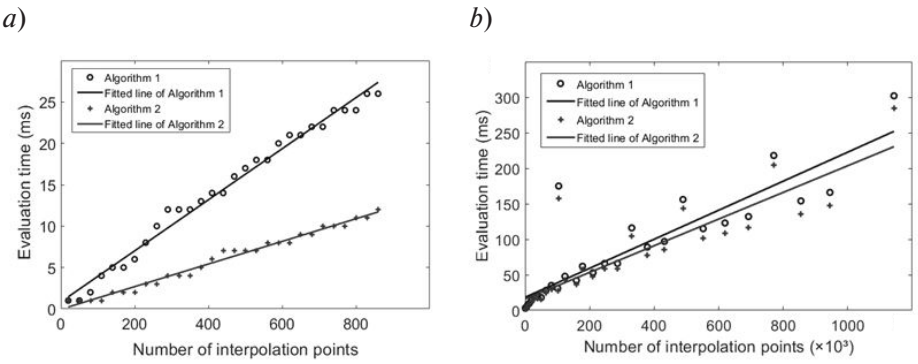

Fig. 7. Time comparison of the two algorithms for cells modeling: *a* – curves; *b* – surfaces

gorithm 1, with *p*-value of 0.6879. Hence, the adoption of Algorithm 2 is an appropriate rapid modeling approach for cytoskeletal curve's visual modeling.

Conclusion

The morphology of rice leaves is directly associated with the number and positional arrangement of cells. The rice cell living system belongs to the scope of micro-modeling. Generally, the modeling is divided into three layers. The bottom layer is a domain layer involving the knowledge field of plant-microbe chemistry. The intermediate layer is a physical mechanism layer that describes biological phenomena. The top layer is a representation layer of changes in cell morphology, which involves computer graphics, informatics, and computing technology, and has important research prospect and application value. This work focuses on the rapid expression method of cell geometric modeling at presentation layer. This work has four major conclusions.

(1) Based on the rational Bernstein basis function extension space, it is easy to obtain new curve and surface shape control variables by changing the affine combination coefficients.

(2) The cytoskeletal curve modeling by the convex combination optimization method (Algorithm 2) proposed in this paper has significant advantage in terms of computation speed over de Casteljau algorithm.

(3) Fixing the control vertex position 3D vectors simulates the deformation of real cell shape by changing the vertex weights (one-dimensional real number), which is beneficial for simplifying the relationship between cell stress and strain.

(4) The visual method in this study has universality in CAGD applications, and is easy to be generalized.

This study was supported by the National Natural Science Foundation of China (Grant No. 61762048; Grant No. 61363041; Grant No. 61562039) and the National Key Research and Development Program of China (Grant No. 2020YFD1100603).

REFERENCES

1. **Xu Jing, Wang Li, Qian Qian, et al.** Research advance in molecule regulation mechanism of leaf morphogenesis in rice (Oryza sativa L.). *ACTA Agronomica Sinica*, 2013, Vol. 39(5), Pp. 767–774. (in Chinese)

2. **Li Qinglin.** *Studies on modeling for the morphological variation of cucumber leaf based on micro-mechanics*. Jiangsu University, 2013. (in Chinese)

3. **Torode T.A., O'Neill R., Marcus S.E., et al.** Branched pectic galactan in phloem-sieve-element cell walls: Implications for cell mechanics. *Plant physiology*, 2018, Vol. 176(2), Pp. 1547–1558.

4. **Yi W., Zhao Y., Wu C., et al.** Algebraic topological method for semantic modelling of plant cell shapes. *2019 XXII International Conference on Soft Computing and Measurements*, St. Petersburg, Russia, 2019, Pp. 176–178, DOI: 10.1109/SCM.2019.8903849

5. **Gao Q., Fang Y., Zhang S., et al.** Dynamic effect of beta-amyloid 42 on cell mechanics. *Journal of Biomechanics*, 2019, No. 86, Pp. 79–88.

6. **Yi W., Zhao Y., Jiang Y., et al.** Computer simulation of plant cell plasmolysis based on physical and mechanical analyses. *2020 IEEE Conference of Russian Young Researchers in Electrical and Electronic Engineering (EIConRus)*, St. Petersburg and Moscow, Russia, 2020, Pp. 560–562. DOI: 10.1109/EIConRus49466.2020.9039139

7. **Marshall W.F.** Introduction to quantitative cell biology. *Colloquium Series on Quantitative Cell Biology*. San Francisco: Morgan & Claypool Life Sciences, 2017, P. 49.

8. **Mogilner A., Allard J., Wollman R.** Cell polarity: Quantitative modeling as a tool in cell biology. *Science*, 2012, Vol. 336(6078), Pp. 175–179.

9. **Avramouli A.** *Validation of modeling and simulation methods in computational biology. GeNeDis*. Springer, Cham, 2020, Pp. 323–330.

10. **Souza N.M., Topham A.T., Bassel G.W.** Quantitative analysis of the 3D cell shape changes driving soybean germination. *Journal of Experimental Botany*, 2017, Vol. 68(7), Pp. 1531–1537.

11. **Earles J.M., Buckley T.N., Brodersen C.R, et al.** Embracing 3D complexity in leaf carbon–water exchange. *Trends in Plant Science*, 2019, Vol. 24(1), Pp. 15–24.

12. **Haas K.T., Wightman R., Meyerowitz E.M., et al.** Pectin homogalacturonan nanofilament expansion drives morphogenesis in plant epidermal cells. *Science*, 2020, Vol. 367(6481), Pp. 1003–1007.

13. **Yang Yan-Hua, Wang Cai-Lin.** Comparative study on the microstructure and ultrastructure for three cultivated varieties of rice. *Bulletin of Botanical Research*, 2010, Vol. 30(2), Pp. 152–156. (in Chinese)

14. **Farin G.** *Curves and surfaces for computer-aided geometric design: A practical guide*. Cambridge: Academic Press, 2014, Pp. 101–288.

15. **Cottrell J.A., Hughes T.J.R., Bazilevs Y.** *Isogeometric analysis: Toward integration of CAD and FEA*. Hoboken: John Wiley & Sons, 2009, Pp. 1–106.

16. **Kobayashi S.** *Differential geometry of curves and surfaces*. Springer, Singapore, 2019.

17. **Farouki R.T., Giannelli C., Sestini A.** New developments in theory, algorithms, and applications for Pythagorean–Hodograph Curves. *Advanced Methods for Geometric Modeling and Numerical Simulation*. Springer, Cham, 2019, Pp. 127–177.

18. **Guo Yu.** *Research on Hermite Interpolation of Quadric Parabolic-PH Curve*. Hefei University of Technology, 2019.

19. **Lu X.J., Zheng J., Cai Y., et al.** Geometric characteristics of a class of cubic curves with rational offsets. *Computer-Aided Design*, 2016, No. 70, Pp. 36–45.

20. **Khan K., Lobiyal D.K.** Bèzier curves based on Lupaş (p, q)-analogue of Bernstein functions in CAGD. *Journal of Computational and Applied Mathematics*, 2017, No. 317, Pp. 458–477.

21. **Kirmani S., Riaz M.B.** Shape preserving fractional order KNR C 1 cubic spline. *The European Physical Journal Plus*, 2019, Vol. 134(7), P. 319.

22. **Asghar M., Mustafa G.** A family of binary approximating subdivision schemes based on binomial distribution. *Mehran University Research Journal of Engineering and Technology*, 2019, Vol. 38(4), Pp. 1087–1100.

23. **Nuntawisuttiwong T., Dejdumrong N.** Fast and efficient algorithms for evaluating uniform and non-uniform Lagrange and Newton curves. *International Journal of Computer and Information Engineering*, 2019, Vol. 13(8), Pp. 448–452.

24. **Beccari C.V., Casciola G.** A Cox-de Boor-type recurrence relation for C1 multi-degree splines. *Computer Aided Geometric Design*, 2019, No. 75, Article 101784.

25. **Toshniwal D., Speleers H., Hiemstra R.R., et al.** Multi-degree B-splines: Algorithmic computation and properties. *Computer Aided Geometric Design*, 2020, No. 76, Article 101792.

26. **Hussain S.M., Rehman A.U., Baleanu D., et al.** Generalized 5-point approximating subdivision scheme of varying arity. *Mathematics*, 2020, Vol. 8(4), P. 474.

27. **Shahzad A., Khan F., Ghaffar A., et al.** A novel numerical algorithm to estimate the subdivision depth of binary subdivision schemes. *Symmetry*, 2020, Vol. 12(1), P. 66.

28. **Woźny P., Chudy F.** Linear-time geometric algorithm for evaluating Bézier curves. *Computer-Aided Design*, 2020, 118: 102760.

29. **Zhao Chun-jiang, Lu Sheng-lian, Guo Xin-yu, et al.** Advances in research of digital plant: 3D Digitization of plant morphological structure. *Scientia Agricultura Sinica*, 2015(17), Pp. 3415–3428. (in Chinese)

30. **Farin G., Josef H., Kim M.-S.** *Handbook of computer aided geometric design*. Elsevier, 2002.

31. **Xiao Bo, Yun Hongxiang, Yang Deyong, et al.** One-dimensional isothermal drying model for parenchyma cell tissue of potato tuber. *Transactions of the Chinese Society of Agricultural Engineering (Transactions of the CSAE)*, 2019, Vol. 35(16), Pp. 309–319. DOI: 10.11975/j.issn.1002-6819.2019.16.034

Received 02.08.2020.

СПИСОК ЛИТЕРАТУРЫ

1. **Xu Jing, Wang Li, Qian Qian, et al.** Research advance in molecule regulation mechanism of leaf morphogenesis in rice (Oryza sativa L.) // ACTA Agronomica Sinica. 2013. Vol. 39(5). Pp. 767–774. (in Chinese)

2. **Li Qinglin.** Studies on modeling for the morphological variation of cucumber leaf based on micro-mechanics. Jiangsu University, 2013. (in Chinese)

3. **Torode T.A., O'Neill R., Marcus S.E., et al.** Branched pectic galactan in phloem-sieve-element cell walls: Implications for cell mechanics // Plant Physiology. 2018. Vol. 176(2). Pp. 1547–1558.

4. **Yi W., Zhao Y., Wu C., et al.** Algebraic topological method for semantic modelling of plant cell shapes // 2019 XXII Internat. Conf. on Soft Computing and Measurements, St. Petersburg, Russia, 2019. Pp. 176–178. DOI: 10.1109/SCM.2019.8903849

5. **Gao Q., Fang Y., Zhang S., et al.** Dynamic effect of beta-amyloid 42 on cell mechanics // J. of Biomechanics. 2019. No. 86. Pp. 79–88.

6. **Yi W., Zhao Y., Jiang Y., et al.** Computer simulation of plant cell plasmolysis based on physical and mechanical analyses // 2020 IEEE Conf. of Russian Young Researchers in Electrical and Electronic Engineering (EIConRus). St. Petersburg and Moscow, Russia, 2020. Pp. 560–562. DOI: 10.1109/EIConRus49466.2020.9039139

7. **Marshall W.F.** Introduction to quantitative cell biology // Colloquium Series on Quantitative Cell Biology. San Francisco: Morgan & Claypool Life Sciences, 2017. P. 49.

8. **Mogilner A., Allard J., Wollman R.** Cell polarity: Quantitative modeling as a tool in cell biology // Science. 2012. Vol. 336(6078). Pp. 175–179.

9. **Avramouli A.** Validation of modeling and simulation methods in computational biology. GeNeDis. Springer, Cham, 2020. Pp. 323–330.

10. **Souza N.M., Topham A.T., Bassel G.W.** Quantitative analysis of the 3D cell shape changes driving soybean germination // J. of Experimental Botany. 2017. Vol. 68(7). Pp. 1531–1537.

11. **Earles J.M., Buckley T.N., Brodersen C.R, et al.** Embracing 3D complexity in leaf carbon–water exchange // Trends in Plant Science. 2019. Vol. 24(1). Pp. 15–24.

12. **Haas K.T., Wightman R., Meyerowitz E.M., et al.** Pectin homogalacturonan nanofilament expansion drives morphogenesis in plant epidermal cells // Science. 2020. Vol. 367(6481). Pp. 1003–1007.

13. **Yang Yan-Hua, Wang Cai-Lin.** Comparative study on the microstructure and ultrastructure for three cultivated varieties of rice // Bulletin of Botanical Research. 2010. Vol. 30(2). Pp. 152–156. (in Chinese)

14. **Farin G.** Curves and surfaces for computer-aided geometric design: A practical guide. Cambridge: Academic Press, 2014. Pp. 101–288.

15. **Cottrell J.A., Hughes T.J.R., Bazilevs Y.** Isogeometric analysis: Toward integration of CAD and FEA. Hoboken: John Wiley & Sons, 2009, Pp. 1–106.

16. **Kobayashi S.** Differential geometry of curves and surfaces. Singapore: Springer, 2019.

17. **Farouki R.T., Giannelli C., Sestini A.** New developments in theory, algorithms, and applications for Pythagorean–Hodograph Curves // Advanced Methods for Geometric Modeling and Numerical Simulation. Springer, Cham, 2019. Pp. 127–177.

18. **Guo Yu.** Research on Hermite Interpolation of Quadric Parabolic-PH Curve. Hefei University of Technology, 2019.

19. **Lu X.J., Zheng J., Cai Y., et al.** Geometric characteristics of a class of cubic curves with rational offsets // Computer-Aided Design. 2016. No. 70. Pp. 36–45.

20. **Khan K., Lobiyal D.K.** Bèzier curves based on Lupaş (p, q)-analogue of Bernstein functions in CAGD // J. of Computational and Applied Mathematics. 2017. No. 317. Pp. 458–477.

21. **Kirmani S., Riaz M.B.** Shape preserving fractional order KNR C 1 cubic spline // The European Physical Journal Plus. 2019. Vol. 134(7). P. 319.

22. **Asghar M., Mustafa G.** A family of binary approximating subdivision schemes based on binomial distribution // Mehran University Research Journal of Engineering and Technology. 2019. Vol. 38(4). Pp. 1087–1100.

23. **Nuntawisuttiwong T., Dejdumrong N.** Fast and efficient algorithms for evaluating uniform and nonuniform Lagrange and Newton curves // Internat. J. of Computer and Information Engineering. 2019. Vol. 13(8). Pp. 448–452.

24. **Beccari C.V., Casciola G.** A Cox-de Boor-type recurrence relation for C1 multi-degree splines // Computer Aided Geometric Design. 2019. No. 75. Article 101784.

25. **Toshniwal D., Speleers H., Hiemstra R.R., et al.** Multi-degree B-splines: Algorithmic computation and properties // Computer Aided Geometric Design. 2020. No. 76. Article 101792.

26. **Hussain S.M., Rehman A.U., Baleanu D., et al.** Generalized 5-point approximating subdivision scheme of varying arity // Mathematics. 2020. Vol. 8(4). P. 474.

27. **Shahzad A., Khan F., Ghaffar A., et al.** A novel numerical algorithm to estimate the subdivision depth of binary subdivision schemes // Symmetry. 2020. Vol. 12(1). P. 66.

28. **Woźny P., Chudy F.** Linear-time geometric algorithm for evaluating Bézier curves // Computer-Aided Design. 2020. No. 118. Article 102760.

29. **Zhao Chun-jiang, Lu Sheng-lian, Guo Xin-yu, et al.** Advances in research of digital plant: 3D Digitization of plant morphological structure // Scientia Agricultura Sinica. 2015(17). Pp. 3415–3428. (in Chinese)

30. **Farin G., Josef H., Kim M.-S.** Handbook of computer aided geometric design. Elsevier, 2002.

31. **Xiao Bo, Yun Hongxiang, Yang Deyong, et al.** One-dimensional isothermal drying model for parenchyma cell tissue of potato tuber // Transactions of the Chinese Society of Agricultural Engineering (Transactions of the CSAE). 2019. Vol. 35(16). Pp. 309–319. DOI: 10.11975/j.issn.1002-6819.2019.16.034

Статья поступила в редакцию 02.08.2020.

THE AUTHOR / СВЕДЕНИЯ ОБ АВТОРЕ

Yi Wenlong
И Вэньлун
E-mail: yiwenlong@jxau.edu.cn

Zhao Yingding
Чжао Индин
E-mail: zhaoyingding@163.com